Article

Polyelectrolyte and Non-Polyelectrolyte Polyacrylamide Copolymer Solutions: the Role of Salt on the Intra- and Intermolecular Interactions

Ana M. S. Maia,[a] Marcos A. Villetti,[b] Redouane Borsali[c,d] and Rosangela C. Balaban[,a]*

[a]*Laboratory of Petroleum Research, Instituto de Química, Universidade Federal do Rio Grande do Norte,
PO Box 1662, 59078-970 Natal-RN, Brazil*

[b]*Laboratório de Espectroscopia e Polímeros, Departamento de Física,
Universidade Federal de Santa Maria, 97105-900 Santa Maria-RS, Brazil*

[c]*Centre de Recherches sur les Macromolécules Végétales (CERMAV-CNRS),
BP 53, F-38041 Grenoble Cedex 9, France*

[d]*Laboratory of Chemistry of Organic Polymers, Ecole nationale supérieure de chimie et de physique
de Bordeaux (ENSCPB), Bordeaux I University, Pessac Cedex, France*

Poli(acrilamida-*co*-dihexilacrilamida) (PAHM-0) e poli(acrilamida-*co*-acrilato de sódio-*co*-dihexilacrilamida) (PAHM-21) foram estudadas por espalhamento de raios-X a baixos ângulos (SAXS), espalhamento de luz (LS) e reologia. Os resultados de SAXS ressaltaram o caráter polieletrolítico da PAHM-21, com uma conformação altamente estendida em solução aquosa devido às repulsões entre as cargas, enquanto a PAHM-0 tem uma conformação em novelo aleatório. As medidas de LS indicaram que a PAHM-0 forma aglomerados intermoleculares em solução, na presença e na ausência de sal, mesmo com um conteúdo hidrofóbico menor que o descrito na literatura para poliacrilamidas associativas. Contudo, os resultados reológicos mostraram que, apesar de haver associação hidrofóbica, não há um aumento da viscosidade. Os resultados de LS da PAHM-21 sugerem que esse polímero forma, predominantemente, associações intramoleculares na presença de sais. Além disso, as medidas viscosimétricas mostram que a sua viscosidade diminui com a blindagem das cargas pela adição de sais.

Poly(acrylamide-*co*-dihexylacrylamide) (PAHM-0) and poly(acrylamide-*co*-sodium acrylate-*co*-dihexylacrylamide) (PAHM-21) were studied through small-angle X-ray scattering (SAXS), light scattering (LS) and rheology. SAXS results highlighted the polyelectrolyte character of PAHM-21, with highly extended conformation in aqueous solution owing to charge repulsion, while the PAHM-0 has a coil conformation. LS measurements indicated that PAHM-0 makes intermolecular clusters in solution, in presence and absence of salt, even with a lower hydrophobic content than that described in the literature to the associative polyacrylamides. However, the rheological results showed that there is not an enhancement of the viscosity although hydrophobic association takes place. LS results for PAHM-21 suggest that this polymer makes intramolecular associations mainly in the presence of salts. Furthermore, the viscosity measurements show that its viscosity decreases due to screening of the charges by the addition of salts.

Keywords: amphiphilic polyacrylamide, polyelectrolyte, slow relaxation mode, cluster, self-diffusion of charged chains

Introduction

Hydrophobically-associating acrylamide-based copolymers with a small number of hydrophobic groups have been extensively studied in previous decades.[1-4] When

*e-mail: balaban@supercabo.com.br

dissolved in an aqueous solution above the concentration of aggregation (C_{agg}), the polymer molecules aggregate to form reversible supermolecular structures via hydrophobic intermolecular association, commonly resulting in a dramatic increase in the apparent viscosity. The degradation upon shearing does not occur and, for specific copolymers, the shear stress could lead to an additional increase in

viscosity.[1,5] The hydrophobic monomers are mainly derivatives of acrylamide, acrylic esters and their derivatives.[6] For some copolymers, the viscosity at low polymer concentration is not high enough for applications such as oil recovery.[7,8]

Acrylamide/*N,N*-dihexylacrylamide copolymers were previously reported.[2,7,9] It was stated that their viscosity depended not only on the presence of hydrophobic groups, but also on the type, concentration and distribution of these groups in the polymer chain. And, although hydrolyzed polyacrylamides have already been analyzed by dynamic light scattering, both in dilute solution[10] as in gel,[11] a study of these polymers and the structures formed in solution, after the introduction of hydrophobic groups, using light scattering, was not done. One of the major interests of our laboratory concerns associating polymers, and in recent years we have focused on the use of different associating polymers such as multisticker polyacrylamides,[3,12,13] surfactant glycopolymers[14] and hydrophobically modified carbohydrates.[15] In the present work, the physicochemical properties of a hydrophobically modified polyacrylamide and its hydrolyzed derivative were studied through SAXS, light scattering and rheology. The effect of ionic strength and shear rate on the aggregates formation was investigated in the semi dilute regime, at C ~ C*. In this work, we show that for the neutral polymer, the intermolecular aggregates are not enough to promote an increase in viscosity, and to the charged polymer, the presence of charges do not permit the observation of clusters even in the presence of salt, but their viscosity is consistent with the polymer expansion.

Experimental

Materials

The chemical structures of the polymers used in this study are shown in Scheme 1. The hydrophobically modified polyacrylamides were named PAHM-0 and PAHM-21, having an average molar mass of 4.9×10^5 and 4.6×10^5 g mol^{-1}, respectively, determined by static light scattering (Zimm plot analysis). PAHM-0 is a neutral polyacrylamide with 0.20 mol% of *N,N*-dihexylacrylamide as hydrophobic group, and PAHM-21 has 0.26 mol% of *N,N*-dihexylacrylamide and 21 mol% of acrylate groups. The method of synthesis, hydrolysis of the hydrophobically modified polyacrylamides, determination of hydrophobic content and hydrolysis degree of the polymers have been previously reported.[12] All solvents and reagents of the best grade available were used without further purification.

The average molar mass and radius of gyration from these polymers were determined early[12] and were used to calculate the critical concentrations (C*), as described in the Supplementary Information (SI) section. The results are C* equal to 0.39 g L^{-1}, at 25 °C in 0.1 mol L^{-1} NaCl for PAHM-0 and 1.85 g L^{-1}, at 25 °C in 1.0 mol L^{-1} NaCl for PAHM-21. Therefore, at lower ionic strength, C* of the evaluated polymers reaches much lower values. This means that all the measurements carried out at 0.5, 2, 10 and 20 g L^{-1} were performed in semi dilute regime. Milli-Q water was used for the preparation of solvents which were filtered through 0.1 μm cellulose acetate Millipore filters. The polymer solutions were prepared by dissolution of a known amount of polymer in the appropriate solvent and, after 96 h of stirring, the solutions were filtered through 0.45 μm cellulose acetate membrane.

Methods

Small-angle X-ray scattering

SAXS experiments were performed at the D11A-SAXS2 beamline of the National Synchrotron Light Laboratory (LNLS) (Campinas-SP, Brazil). A two-dimensional position sensitive detector (MAR-165) (area of 16 cm^2) was used for these experiments and a wavelength of the monochromatic beam of 1.488 Å. The scattering patterns were collected
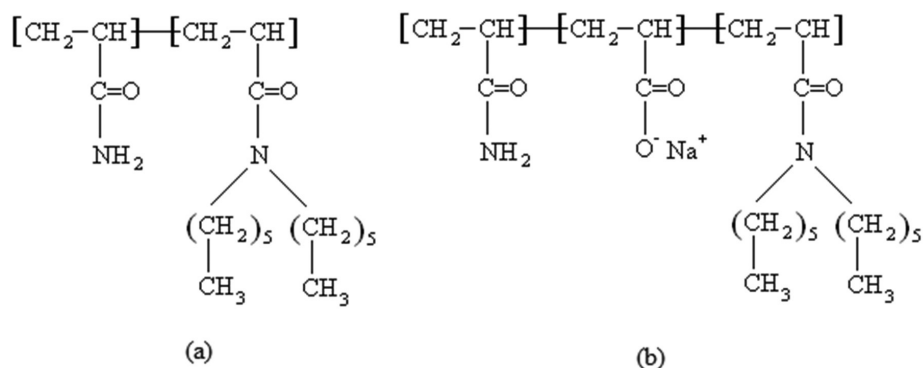
Scheme 1. Chemical structures of (a) PAHM-0 and (b) PAHM-21.

after an exposure time of 300 s. To cover the *q* range from 0.01 to 0.23 Å^{-1}, the sample detector distance was set to 1413.9 mm. The samples were placed in a stainless steel sample holder closed by two mica windows, normal for the beam, and the sample cell was introduced to a chamber connected to a vacuum to decrease the parasitic scattering. A thermal bath was used to maintain the temperature at 25 °C. The pure solvent scattering was subtracted from the total intensity and the scattering profiles were corrected for sample absorption and detector response. The studied polymer concentrations were 10 and 20 g L^{-1}.

Light scattering

Static (SLS) and dynamic (DLS) light scattering measurements were performed at the Laboratory of Chemistry of Organic Polymers, Bordeaux I University (Pessac Cedex-France) with an automatic goniometer (ALV model/58-125 S/N 91) equipped with multiple τ correlator and a He-Ne laser source operating at l 632.8 nm (22 mW power). For static light scattering, the data points were taken at angles between 40º and 130º, at 25 °C and polymer concentration of 0.5 g L^{-1}.

For DLS, the data points were taken at angles between 30° and 150°, at 25 °C and polymer concentration of 2 g L^{-1}. The homodyne intensity correlation function $G^{(2)}(t)$ was measured within the range of delay times from 10^{-4} to 10^{5} ms. The normalized homodyne intensity correlation function $g^{(2)}(t)$ is related to the normalized electric field time correlation function $g^{(1)}(t)$ by Siegert relation (equation 1)[16]

$$g^{(2)}(t) = 1 + \beta \left| g^{(1)}(t) \right|^2 \qquad (1)$$

where $g^{(2)}(t) = G^{(2)}(t)/G^{(2)}(\infty)$, $G^{(2)}(\infty)$ is an experimentally determined baseline and β is the optical coherence factor. The correlation functions were analyzed by the software provided with the equipment, through inverse Laplace transformation using the constrained regularization (CONTIN) method developed by Provencher[17] and some representative examples of the normalized field autocorrelation functions are given in the SI section. For each correlation function, a relaxation time distribution was obtained using: a DLS-Exponential ($g^{(2)}(t)$) fit model; 200 ns as the first datapoint and 93.95 s as the last datapoint; minimum decay time of 0.001 ms and maximum decay time of 1000 ms and 150 grid points.

The value of relaxation time (τ) in each peak of the relaxation time distribution was determined and a spreadsheet was used to construct a table with each analyzed angle (θ) in radians, the correspondents scattering wavevector (*q*), squared scattering wavevector (*q²*), cubic scattering wavevector (*q³*), relaxation time (τ) and

relaxation rate (Γ = 1/τ). The values of Γ were plotted as a function of *q* and the *q*-dependence was determined. Then, Γ was plotted as function of *q²* and extrapolated to *q* → 0. The obtained angular coefficient is the diffusion coefficient ($D_{q\to0}$). $D_{q\to0}$ could be related to the hydrodynamic radius (R_h) (equation 2), or to the dynamic correlation length (ξ_D) (equation 3), through the Stokes-Einstein relation[18-20]

$$D_0 = \frac{k_B T}{6\pi\eta_0 R_h} \qquad (2)$$

$$D_0 = \frac{k_B T}{6\pi\eta_0 \xi_D} \qquad (3)$$

where k_B is Boltzmann's constant, T is absolute temperature and η is the medium viscosity.

Viscosity measurements

Viscometric properties of PAHM-0 solutions at concentration of 2 g L^{-1} were measured by an automatic Ubbelohde capillary viscometer (diameter capillary 0.46 mm, Schott-Gerate) with automatic dilution (Tritonic T110), immersed in a water bath maintained at 25.0 ± 0.1 °C. Due to their higher viscosity, the PAHM-21 was analyzed using a Haake MARS rotational rheometer from Thermo Scientific, equipped with concentric cylinder system and a DC50 thermostatic bath, at shear rate of 100 s^{-1} and at the same temperature and concentration conditions of PAHM-0.

Results and Discussion

PAHM-21 is a partially hydrolyzed and hydrophobically modified polyacrylamide. The presence of charges on PAHM-21 chains significantly modifies their conformation with respect to the neutral polymer (PAHM-0). The polyelectrolyte character of PAHM-21 was investigated through SAXS in the semi dilute regime. For PAHM-21, a scattering peak in the *q*-SAXS range was observed and the peak position depends on polymer concentration. This behavior is illustrated in Figure 1, in which scattering intensity normalized by polymer concentration is plotted as a function of *q*. The results show that the position of the wavevector at maximum scattering intensity q_{max} is shifted towards higher scattering vector values with the increase in the polymer concentration.

In the semi dilute regime, the more accepted explanation for the polyelectrolyte correlation peak is the isotropic model by de Gennes *et al.*[21] In the isotropic model, the polyelectrolyte chains break up into a series of "electrostatic blobs," each of size ξ_e. For a spatial scale (r)
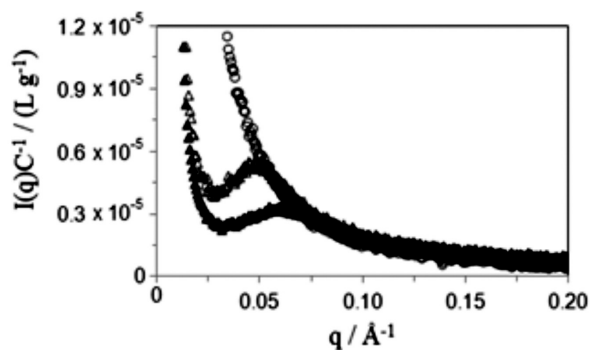
Figure 1. I(q)/C *vs. q* for PAHM-0 (circle) and PAHM-21 (triangle) at polymer concentrations of 10 g L^{-1} (open symbol) and 20 g L^{-1} (full symbol), in Milli-Q water at 25 °C.

less than ξ_e (r < ξ_e), the thermal energy dominates over electrostatic, and the chain conformation is a self-avoiding walk in a good solvent.[22] Otherwise, for r larger than ξ_e (r > ξ_e), the electrostatic interaction dominates thermal energy, therefore, the chains of electrostatic blobs are stiff locally (a directed random walk) due to strong charge repulsion, leading to structured solution in the semi dilute regime, so that, the distance to the nearest chain is quite close to the correlation length (ξ).[23] ξ can be determined directly from q_{max} in accordance to Bragg's equation ($\xi = 2\pi/q_{max}$). Therefore, electrostatic repulsion between neighboring PAHM-21 chains on salt-free solutions is the reason there is a peak in SAXS profile.

For PAHM-21, the curves in SAXS suggest that ξ decreases with an increase in polymer concentration, as expected for charged polymers. These SAXS results highlight the polyelectrolyte character of PAHM-21. Figure 1 also shows the behavior of the hydrophobically modified polyacrylamide (PAHM-0). For this polymer, the ratio I(q)/C decreases with the increase in q value. As expected, in the q-SAXS range, no scattering peak was observed because PAHM-0 is a neutral polymer. These results clearly show that in the semi dilute regime, PAHM-0 has a coil conformation, while for PAHM-21, the electrostatic blobs are highly extended owing to charge repulsion. As can be seen below, this rigid conformation adopted by polyelectrolyte is the cause of high viscosity of PAHM-21 at low ionic strength, when compared to PAHM-0.

Before starting the study of the aggregation phenomenon, the salt concentration in which the ionic charges onto PAHM-21 are screened (0.2 mol L^{-1}) was selected through SLS. Figure 2 shows the curves of absolute time-average light scattering intensity excess (Rayleigh ratio, R$_\theta$) *vs. q* for PAHM-21 at 0.5 g L^{-1} and different NaCl concentration. R$_\theta$ is given by equation 4. As can be seen in the wavevector range (q-SLS) studied when no salt is added, R$_\theta$ is quite feeble, i.e., just above the solvent

scattering level. Otherwise, the intensity of the scattered light markedly increases with ionic strength, as expected for polyelectrolyte solutions.

$$R_\theta = \frac{i_{solution} - i_{solvent}}{i_{toluene}} R_{\theta\, toluene} \qquad (4)$$

where $i_{solution}$, $i_{solvent}$ and $i_{toluene}$ mean the intensity of light scattered by the solution, by the solvent, and by the toluene (standard), respectively.
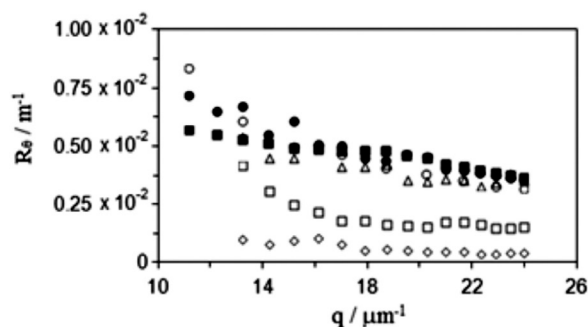
Figure 2. Intensity of scattered light as a function of q for PAHM-21 at 0.5 g L^{-1} to different NaCl concentrations at 25 °C: ($\diamond$) 0 mmol L^{-1}, ($\square$) 10 mmol L^{-1}, ($\triangle$) 50 mmol L^{-1}, ($\bigcirc$) 0.1 mol L^{-1}, ($\blacksquare$) 0.2 mol L^{-1} and ($\bullet$) 2 mol L^{-1}.

The results observed in Figure 2 are experimental evidence of the osmotic incompressibility of PAHM-21 solution at low ionic strength. The Rayleigh ratio (R$_\theta$) at $q \rightarrow 0$ is directly proportional to the osmotic compressibility of the solution (dπ/dc)$^{-1}$ in accordance with equation 5. When the ionic strength is close to zero, the osmotic compressibility is low due to the high rigidity of the polyelectrolyte in solution, and the fluctuation in the concentration is small, thus a weak scattering is observed. Figure 2 also shows that in a salt concentration equal to or higher than 50 mmol L^{-1} (ionic strength of 5×10^{-2} mol L^{-1}), there is not a large increase in the light scattering intensity, meaning that the negative charges on hydrolyzed polymer are screening out.[24]

$$\frac{Kc}{\Delta R_\theta (q \rightarrow 0)} = \frac{1}{RT}\left(\frac{\partial\pi}{\partial c}\right) \qquad (5)$$

DLS measurements were performed for aqueous PAHM-0 and PAHM-21 solutions, at 2 g L^{-1} (C ~ C*), in the presence of different salt concentrations (ionic strength from 0 to 0.2 mol L^{-1}), at 25 °C. Some examples of the relaxation time distributions are given in Figure 3. As can be seen, both polymers showed a fast and a slow relaxation mode, and it is possible to observe that the salt addition shifts the peak positions and peak intensities. The observed effect

depends on the ionic strength investigated. In the chosen examples, it is possible to observe that at ionic strength of 2.70×10^{-3} mol L^{-1}, both peaks are shifted to higher decay times (Figures 3b and 3e) in relation to the results in absence of salt (Figures 3a and 3d). While at a higher ionic strength, as 2.0×10^{-1} mol L^{-1}, the peaks related to the fast relaxation mode become more intense and the peaks related to the slow relaxation mode shift to the lowest decay times.

It is worth mentioning that the existence of a slow relaxation mode in semi dilute regime was questioned by many researchers. However, Li *et al.*[19,25] through careful DLS experiments on polystyrene solutions have demonstrated its existence. They showed that in an athermal solvent, such as benzene for polystyrene, there is only a single mode of relaxation, even when the concentration is above C*. But in a thermodynamically weaker solvent, such as cyclohexane for polystyrene above the C*, there are two modes of relaxation. They convincingly demonstrated that the slow

mode is real and not an artifact, as previously suggested. The fast and slow relaxation modes may have different origins. For example, Brown and Nicolai[20] attributed the fast mode to collective motions of a transient network, and the slow mode of linear polymers in poor and moderately good solvents to an effect of topological constraints. Whereas Li *et al.*[19,25] attributed the slow mode to transient clusters formed due to the solvent quality.[19,25] Other interpretations of the slow mode can be found in the literature.[26] The relaxation rate (Γ) may present different dependences on the wavevector, according to the origin of the relaxation mode. A q-independent relaxation is generally attributed to a structural relaxation of a network such as observed in permanent or transient gels,[27-29] q^2-dependence is attributed to diffusive motions[28,30] and q^3-dependence is associated with internal motions of temporal domains related to a transient network, when the q-values are large enough to observe these motions.[29]
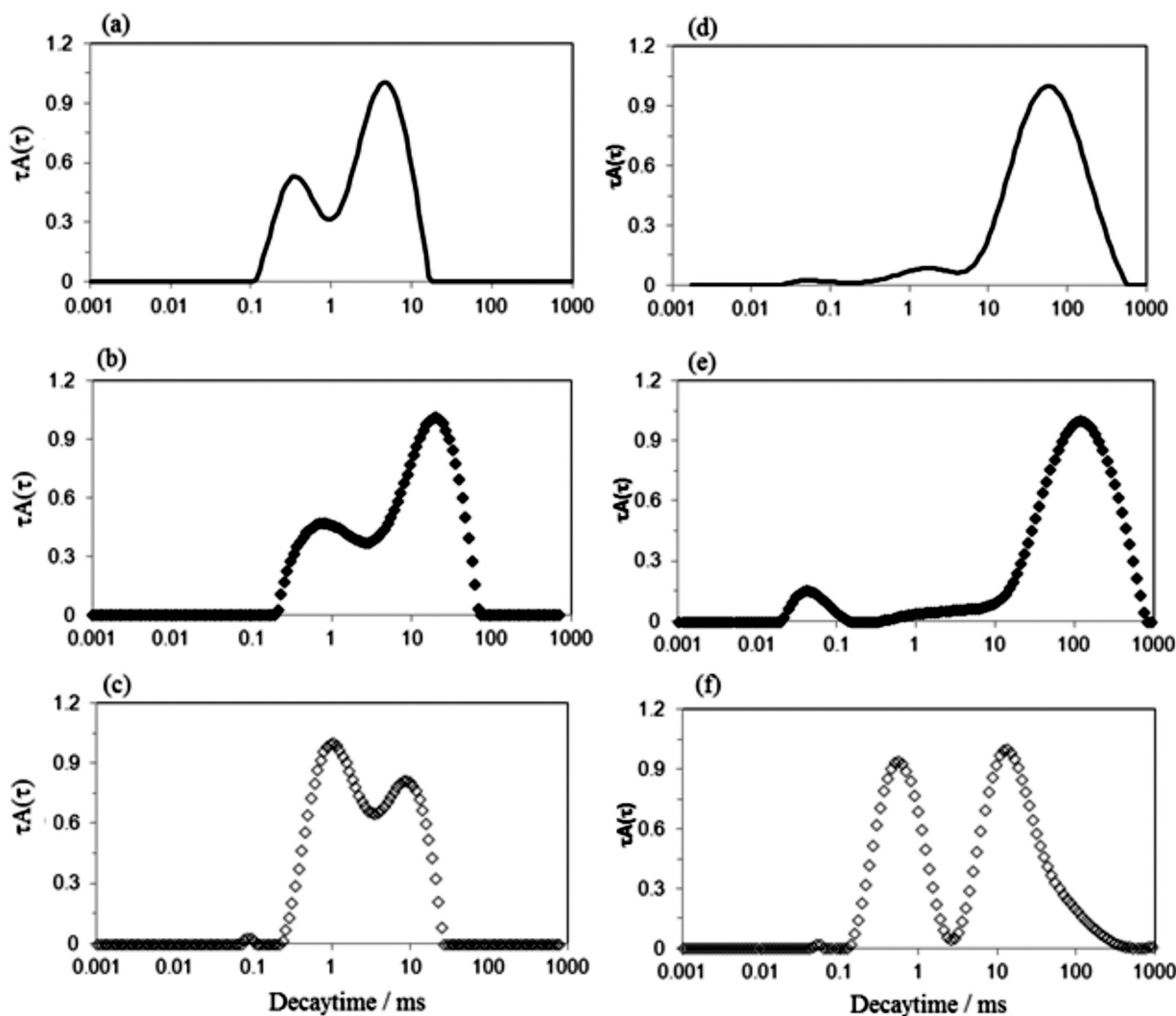
Figure 3. Relaxation time distributions obtained at angle of 60° and diferent ionic strengths. PAHM-0: (a), (b) and (c); PAHM-21: (d), (e) and (f). Ionic strength (–) 0; (◆) 2.70×10^{-3} and (◇) 2.0×10^{-1} mol L^{-1}. Salts: open symbols NaCl and full symbols CaCl$_2$. Polymer concentration: 2 g L^{-1}.

In this last case, it is possible to observe a gradual transition between two limiting regimes: a hydrodynamic regime at small values of the wavevector in which the relaxation mode reflects diffusive motions (Γ is q^2-dependent),[20,30] and at large wavevectors, a non-diffusive slow q-independent mode in a semi dilute theta system[20] or a non-diffusive q^3-dependent regime in a poor solvent.[30] The latter behavior can be observed for the slow mode through a plot of Γ normalized by $\sin^3(\theta/2)$ as a function of $\sin^2(\theta/2)$, as shown for PAHM-0 and PAHM-21 at large wavevectors in Figures 4 and 6. It is possible to observe the ionic effect on the q-dependence. For PAHM-0, in absence of salt, the scattering is q^2-dependent (diffusive) at small angles and q^3-dependent (non-diffusive) at intermediate and large angles for the slow relaxation modes. The addition of salts to the PAHM-0 solutions decreases the diffusive character of it, as can be seen in the examples shown in Figure 4.
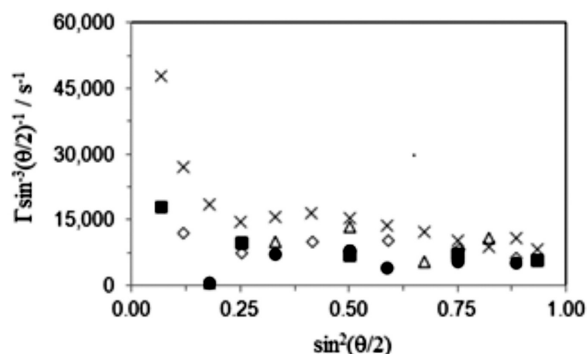

Figure 4. Relaxation rates for the slow mode normalized with $\sin^3(\theta/2)$ as a function of $\sin^2(\theta/2)$ for PAHM-0 at 2 g L^{-1}. Ionic strengths: (×) 0 (distilled water), (■) 5.40×10^{-3}, (△) 1.37×10^{-2}, (●) 4.35×10^{-2} and (◇) 2.0×10^{-1} mol L^{-1}. Salts: open symbols NaCl and full symbols CaCl$_2$.

Due to the presence of the dihexylacrylamide groups, even distilled water is not a good solvent for PAHM-0 and intramolecular and intermolecular hydrophobic interactions can happen, leading to the formation of transient clusters. The fast mode observed in the DLS may be attributed to the fluctuation motion inside the blobs of the transient network into these clusters. The q^2-dependence of these motions indicates their diffusive behavior, and from these results, the $D_{q \to 0}$ was determined in distilled water, using the range of 30° to 60°, in which the q^2-dependence was observe. The values of Γ were plotted as a function of q^2 (SI section). The plots were extrapolated to $q = 0$, and $D_{q \to 0}$ for the fast and slow modes were obtained from the angular coefficients being 1.15×10^{-7} and 1.34×10^{-8} cm^2 s^{-1}, respectively. With these values, the Stokes-Einstein equation gives correlation lengths (ξ) of 21 and 183 nm for the fast and slow modes, respectively. Another indication that the fast and slow modes are diffusive is that ξ does not change with the scattering angle (SI section).[29]

The q^3-dependence observed at large angles could be associated with internal relaxation of temporal hydrophobic domains into the clusters. It is interesting to remember here that a q-independent mode is not expected since the analyzed solutions are in a sol state and not in a gel, as can be observed later in the viscometric results. The diffusive mode is observed at low angles, and the non-diffusive mode (internal relaxation of cluster) is observed at large angles. Adding salt to PAHM-0 solution promotes a transition from Γq^2-dependent to Γq^3-dependent (Figure 4). The progressive change from a diffusive to a non-diffusive regime could be attributed to an increase in the lifetime of the hydrophobic junctions with an increase of salt concentration, as well as to the timescale of the experiment. In both cases, the material would behave as a temporary network.

Relaxation rates as function of ionic strength for the fast and slow modes are shown in Figure 5. It is possible to observe that the Γ values for both modes, measured at an angle higher than 90° (not diffusive) do not change significantly with the ionic strength, while the relaxation rate measured at an angle lower than 90° (diffusive) increases with the ionic strength. This result is another indication that the addition of salt decreases the solvent quality and as a result the hydrophobic interactions are enhanced, leading to a decrease in ξ of the blobs (fast mode) and of the transient clusters (slow mode). These results are in agreement with those shown in Figure 3.

After the analysis of PAHM-0 in absence and presence of salt by DLS, PAHM-21 was characterized at the same conditions. As noted earlier through SAXS and SLS measurements, PAHM-21 behaves as a polyelectrolyte in salt-free aqueous solution, and at 2 g L^{-1}, there are two relaxation modes in absence and presence of salt (Figure 3d-3f). In the literature, different assignments have been made to these relaxation modes. The dynamic of a poly(styrenesulfonate) sodium salt in aqueous solutions was studied in a similar ionic strength range (3×10^{-3} to 7×10^{-1} mol L^{-1}), and it was observed that the polymer solution showed only one relaxation mode at ionic strength higher than 0.2 mol L^{-1} and two modes below this ionic strength. The authors attributed the fast mode to the response of an osmotically stiff system to spontaneous fluctuations and the slow mode to the multimacroion with a loose structure.[24] Other researchers suggest that the origins of the fast mode in polyelectrolyte solutions can be attributed to the coupled diffusion originated from a convective current generated by an induced electric field arising from fluctuation of all charged species (charges on the chain and counterions) in the solution in a short time or length scale. Concerning the slow relaxation mode, it is frequently correlated to the self-diffusion of individual
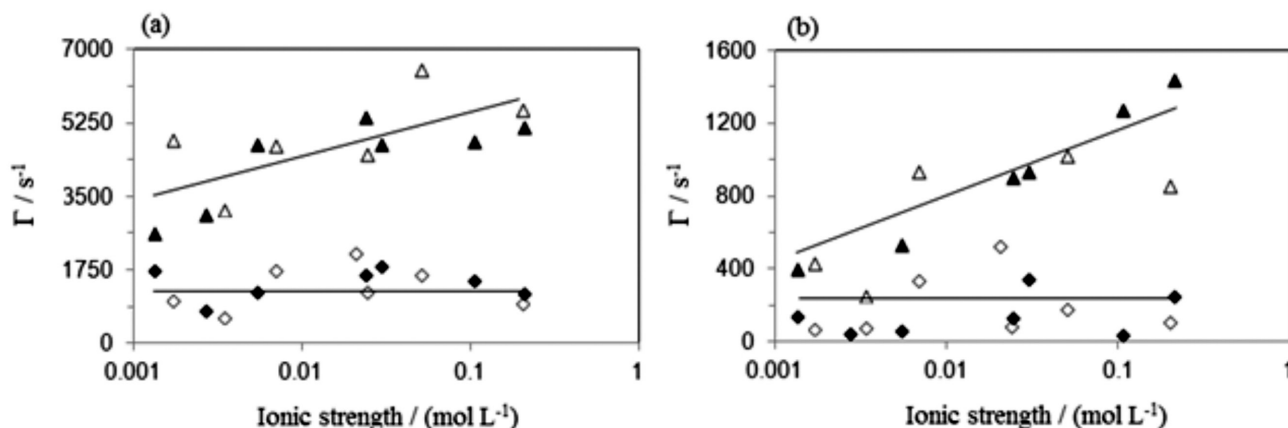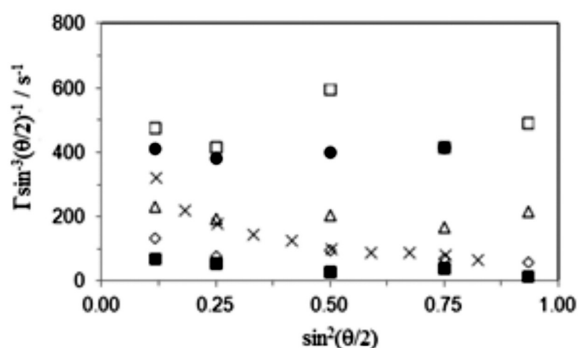
Figure 5. Relaxation rate as a function of the ionic strength for PAHM-0 at 2 g L^{-1}: (a) fast mode; (b) slow mode; (triangle) measures done at an angle of 60°; (diamond) measures done at an angle of 120°; Open symbols: NaCl; Full symbols CaCl$_2$. The lines are guides for the eyes.

chains retarded by surrounding chains in a long time or length.[19,31]

Peitzsch *et al.*[32] suggest that the slow mode in polyelectrolyte solutions corresponds to a non-equilibrium state of the polymer, such as stable aggregates. While Sedlák[33] considers that the slow mode in polyelectrolyte solutions is due to the presence of large multichain domains or temporal aggregates and not due to impurities or aggregates resultant of incomplete polymer solubility.[33] Blanco *et al.*[29] consider that the behavior of this slow mode depends on the specific conditions of a particular system and that temporal domains would induce the appearance of a diffusive mode at small angles. This diffusive behavior, for the slow mode, is observed in Figure 6 for PAHM-21 in distilled water, at angles lower than 70°, and the corresponding $D_{q\to0}$ is 1.27×10^{-9} cm^2 s^{-1}. The correlation length distribution as a function of the scattering angle (SI section) also gives an indication that the fast and slow modes are non-diffusive.[29]

The slow mode becomes q^3-dependent with the salt addition. Blanco *et al.*[29] observed gelatin solutions in which it was only possible to observe the q^2-dependence at low


Figure 6. Relaxation rates for the slow mode normalized with sin^3(q/2) as a function of sin^2(q/2) for PAHM-21. Ionic strengths: (×) 0 (distilled water), (■) 1.35×10^{-3}, (◇) 3.40×10^{-3}, (●) 1.20×10^{-2}, (△) 5.00×10^{-2}, (◆) 1.05×10^{-1} and (□) 2.0×10^{-1} mol L^{-1}. Salts: open symbols NaCl and full symbols CaCl$_2$.

angles and the q^3-dependence at large angles in systems of low rigidity, and the q^3-dependence was detected even in good solvents.[29] In our case, the q^3-dependence could be associated with the reinforcement of the temporal junctions of a transient network by charge screening and induction of hydrophobic associations.

The plots of Γ as a function of ionic strength (Figure 7) for PAHM-21 have a different profile from that of the non-charged polymer plots (Figure 5). For the fast mode (Figure 7a), while Γ measured at an angle higher than 90° varies around an average value, in the same manner as for PAHM-0, Γ measured at an angle lower than 90° is very scattered, not showing a trend. For the slow relaxation mode (Figure 7b), it is possible to observe an increase in the Γ value with the increase of ionic strength at low and high angles. This increase means that the time needed for the polymer to relax declines with ionic strength probably due to the screening of the charges by the cations, leading to a more flexible conformation of the polymer chains in solution. It is also possible to observe that, for measurements carried out in NaCl solutions, the increase in Γ becomes more evident at ionic strength higher than 5×10^{-2} mol L^{-1}. This ionic strength (indicated in the plot by an arrow), was identified by SLS as the ionic strength in which PAHM-21 charges are completely screened.

Although the presence of large clusters to PAHM-0 has been observed, and especially at low ionic strength, its reduced viscosity does not change in all studied salt ranges (Figure 8). At first, these results appear contradictory because the reduced viscosity is directly related to the hydrodynamic volume of the sample. However, if one takes into consideration that the nominal shear rates during the capillary flow calculated for our samples is between 1259 and 2269 s^{-1} (SI section),[34] one can assume that this shear is sufficient to overcome the strength of hydrophobic intermolecular association holding the polymer chains
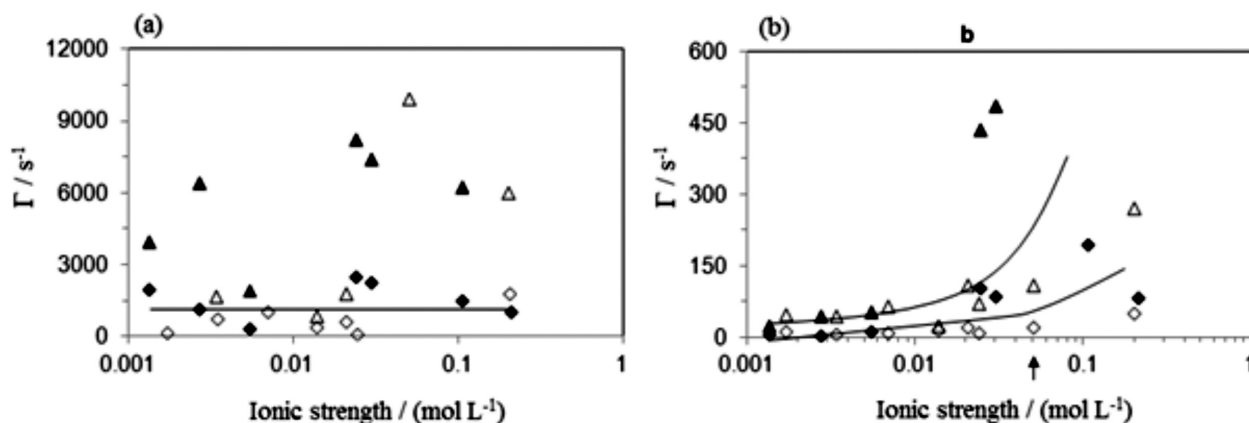
Figure 7. Relaxation rate as a function of the ionic strength for PAHM-21 at 2 g L^{-1}: (a) fast mode; (b) slow mode; (triangle) measures done at an angle of 60°; (diamond) measures done at an angle of 120°; Open symbols: NaCl; Full symbols $CaCl_2$. The lines are guides for the eyes.
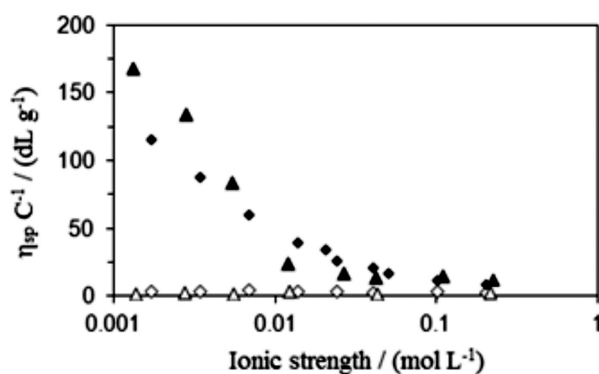
Figure 8. Reduced viscosity as function of ionic strength to PAHM-0 (open symbol), and PAHM-21 (full symbol) at 2 g L^{-1} in presence of different salt at 25 ºC: NaCl (diamond) and $CaCl_2$ (triangle).

together in clusters. Thus, the measured reduced viscosity is related to the viscosity of free chains, and not to clusters.

Comparing the viscosities of PAHM-0 and PAHM-21, it can be observed that even with a smaller average molar mass, PAHM-21 has a viscosity greater than PAHM-0 at low ionic strength. This is due to repulsion between the negative charges present in the polyelectrolyte which are not completely screened at low ionic strength. These results agree with the SAXS measurements, which show the expansion of the PAHM-21 chains. Moreover, the results of viscometry from PAHM-21 are in perfect agreement with those obtained by SLS and DLS. It is possible to observe that the reduced viscosity decreases with increasing salt concentration due to the screening of the charge and consequent reduction of hydrodynamic volume of the polymer.

Conclusion

We have examined the association behavior of two amphiphilic copolymers in aqueous solution. The polymers are statistically modified polymers of acrylamide and

dihexylacrylamide (PAHM-0), and acrylamide, sodium acrylate and dihexylacrylamide (PAHM-21). SAXS results highlighted the conformation adopted by polymers in the semi dilute regime. PAHM-0 shows a coil conformation, while PAHM-21 shows highly extended conformation owing to charge repulsion. Furthermore, static light scattering showed that PAHM-21 in absence of salt presents a typical polyelectrolyte behavior, i.e., a weak light scattering intensity in the semi dilute regime due to low osmotic compressibility. This behavior is in line with SAXS results. In the presence of salt, PAHM-21 shows a high light scattering typical of a neutral polymer.

From DLS results, a more intricate picture emerges. Both polymers show two relaxation modes in the absence and presence of salt (NaCl and $CaCl_2$). The fast relaxation mode from PAHM-0 may be attributed to cooperative diffusion of chain segments between two entanglement points, with ξ of 21 nm. The slow relaxation mode was related to the diffusion of transient clusters observed at small angles, and the internal motions of these transient clusters observed at large angles. The ξ calculated for the scattering at small angles is of 183 nm. The q-dependence of Γ is an indication that the strength of intermolecular hydrophobic interactions are not so strong. This conclusion is reinforced by the results of viscometry. For PAHM-0, the rheological results showed that there is not an enhancement of viscosity, even when formation of polymer clusters in presence of salt was detected by DLS. It probably happens due to the fact that, at high shear rates, solutions consist of individual chains.

For PAHM-21, the fast relaxation mode can be also attributed to chain segments between two entanglement points and the slow relaxation mode at small angles may be attributed to self diffusion of polyelectrolyte chains retarded by interchain friction. A continuous addition of salt increases the Γ due to the decrease of the charge density of

the polyelectrolyte. As expected, the increase in relaxation rate value is accompanied by the decrease of viscosity.

Acknowledgments

Supplementary Information

Supplementary data are available free of charge at http://jbcs.sbq.org.br as a PDF file.

References

1. McCormick, C. L.; Nonaka, T.; Johnson, C. B.; *Polymer* **1988**, *29*, 731.

2. Candau, F.; Selb, J.; *Adv. Colloid Interface Sci.* **1999**, *79*, 149.

3. Maia, A. M. S.; Borsali, R.; Balaban, R. C.; *Mater. Sci. Eng., C* **2009**, *29*, 505.

4. Gouveia, L. M.; Muller, A. J.; *Rheol. Acta* **2009**, *48*, 163.

5. McCormick, C. L.; Middleton, J. C.; Cummins, D. F.; *Macromolecules* **1992**, *25*, 1201; Feng, Y.; Grassl, B.; Billon, L.; Khoukh, A.; François, J.; *Polym. Int.* **2002**, *51*, 939.

6. Feng, Y.; Billon, L.; Grassl, B.; Khoukh, A.; François, J.; *Polymer* **2002**, *43*, 2055; Bastiat, G.; Grassl, B.; François, J.; *Colloid Interface Sci.* **2005**, *289*, 359; Biggs, S.; Hill, A.; Selb, J.; Candau, F.; *J. Phys. Chem.* **1992**, *96*, 1505.

7. Volpert, E.; Selb, J.; Candau, F.; *Macromolecules* **1996**, *29*, 1452.

8. Gao, B.; Jiang, L.; Kong, D.; *Colloid Polym. Sci.* **2007**, *285*, 839.

9. Candau, F.; Regalado, E. J.; Selb, J.; *Macromolecules* **1998**, *31*, 5550; Volpert, E.; Selb, J.; Candau, F.; Green, N.; Argillier, J. F.; Audibert, A.; *Langmuir* **1998**, *14*, 1870; Jiménez-Regalado, E.; Selb, J.; Candau, F.; *Macromolecules* **1999**, *32*, 8580; Jiménez-Regalado, E.; Selb, J.; Candau, F.; *Langmuir* **2000**, *16*, 8611; Jiménez-Regalado, E. J.; Cadenas-Pliego, G.; Pérez-Álvarez, M.; Hernández-Valdez, Y.; *Polymer* **2004**, *45*, 1993; Kujawa, P.; Audibert-Hayet, A.; Selb, J.; Candau, F.; *Macromolecules* **2006**, *39*, 384.

10. Jamieson, A. M.; Presley, C. T.; *Macromolecules* **1973**, *6*, 358.

11. Tanaka, T.; Hocker, L. O.; Benedek, G. B.; *J. Chem. Phys.* **1973**, *59*, 5151.

12. Maia, A. M. S.; Villetti, M. A.; Vidal, R. R. L.; Borsali, R.; Balaban, R. C.; *J. Braz. Chem. Soc.* **2011**, *22*, 489.

13. Maia, A. M. S.; Garcia, R. B.; *Polímeros* **2007**, *17*, 76; Maia, A. M. S.; Costa, M; Borsali, R.; Garcia, R. B.; *Macromol. Symp.* **2005**, *229*, 217.

14. Borges, M. R.; Santos, J. A.; Vieira, M.; Balaban, R.; *Mater. Sci. Eng., C* **2009**, *29*, 519; Borges, M. R.; Balaban, R.; *Macromol. Symp.* **2007**, *258*, 25.

15. Alves, K. S.; Vidal, R. R. L.; Balaban, R. C.; *Mater. Sci. Eng., C* **2009**, *29*, 641; Vidal, R. R. L.; Balaban, R.; Borsali, R.; *Polym. Eng. Sci.* **2008**, *48*, 2011; Silva, S. S.; Menezes, S. M.; Garcia, R. B.; *Eur. Polym. J.* **2003**, *39*, 1515; Marques, N. N.; Curti, P. S.; Maia, A. M. S.; Balaban, R. C.; *J. Appl. Polym. Sci.* **2013**, *129*, 334.

16. Siergert, A. J.; *MIT Rad. Lab. Rap.* **1943**, 465; Chu, B.; *Laser Light Scattering: Application of Photon Correlation Spectroscopy*; Academic Press: London, UK, 1991.

17. Provencher, S. W.; *Comput. Phys. Commun.* **1982**, *27*, 213; Provencher, S. W.; *Comput. Phys. Commun.* **1982**, *27*, 229.

18. Pecora, R.; *Dynamic Light Scattering: Applications of Photon Correlation Spectroscopy*, 1st ed.; Plenum Press: New York, USA, 1985.

19. Li, J.; Li, W.; Huo, H.; Luo, S.: Wu, C.; *Macromolecules* **2008**, *41*, 901.

20. Brown, W.; Nicolai, T.; *Colloid Polym. Sci.* **1990**, *268*, 977.

21. De Gennes, P. G.; Pincus, P.; Velasco, R. M.; Brochard, F.; *J. Phys.* **1976**, *37*, 1461; De Gennes, P. G.; *Scaling Concepts in Polymer Physics*; Cornell University Press: Ithaca, New York, USA, 1979.

22. Dobrynin, A. V.; Colby, R. H.; Rubinstein, M.; *Macromolecules* **1996**, *28*, 1859.

23. Dou, S.; Colby, R. H.; *Macromolecules* **2008**, *41*, 6505.

24. Cong, R.; Temyanko, E.; Russo, P.; Edwin, N.; Uppu, R. M.; *Macromolecules* **2006**, *39*, 731.

25. Li, J.-F.; Lu, Y.-J.; Zhang, G.-Z.; *Chin. J. Polym. Sci.* **2008**, *26*, 465.

26. Vyshivannaya, O. V.; Laptinskaya, T. V.; *Polym. Sci., Part A: Polym. Chem.* **2012**, 364.

27. Adam, M.; Delsanti, M.; *Macromolecules* **1985**, *18*, 1760; Brown, W.; Stepanek, P.; *Macromolecules* **1993**, *26*, 6884.

28. Brown, W.; Stepanek, P.; *Macromolecules* **1992**, *25*, 4359.

29. Blanco, M. C.; Leisner, D.; Vázques, C.; López-Quintela, M. A.; *Langmuir* **2000**, *16*, 8585.

30. Melnichenko, Y. B.; Brown, W.; Rangelov, S.; Wignall, G. D.; Stamm, M.; *Phys. Lett. A* **2000**, *268*, 186.

31. Li, J.; Ngai, T.; Wu, C.; *Polym. J.* **2010**, *42*, 609.

32. Peitzsch, R. M.; Burt, M. J.; Reed, W. F.; *Macromolecules* **1992**, *25*, 806.

33. Sedlák, M.; *J. Chem. Phys.* **1994**, *101*, 10140.

34. Chhabra, R. P., Richardson, J. F.; *Non-Newtonian Flow and Applied Rheology*: *Engineering, Applications*, 2nd ed.; Elsevier, 2008, available at: http://www.sciencedirect.com/science/article/pii/B9780750685320000020 accessed in February 2012.

Supplementary Information

Polyelectrolyte and Non-Polyelectrolyte Polyacrylamide Copolymer Solutions: the Role of Salt on the Intra- and Intermolecular Interactions

Ana M. S. Maia,[a] Marcos A. Villetti,[b] Redouane Borsali[c,d] and Rosangela C. Balaban*,[a]

[a]*Laboratory of Petroleum Research, Instituto de Química, Universidade Federal do Rio Grande do Norte, PO Box 1662, 59078-970 Natal-RN, Brazil*

[b]*Laboratório de Espectroscopia e Polímeros, Departamento de Física, Universidade Federal de Santa Maria, 97105-900 Santa Maria-RS, Brazil*

[c]*Centre de Recherches sur les Macromolécules Végétales (CERMAV-CNRS), BP 53, F-38041 Grenoble Cedex 9, France*

[d]*Laboratory of Chemistry of Organic Polymers, Ecole nationale supérieure de chimie et de physique de Bordeaux (ENSCPB), Bordeaux I University, Pessac Cedex, France*

The critical concentration (C^*) was calculated using the following equation:

$$c^*_{R_g} = \frac{3M_W}{4\pi N_A R_g^3} \qquad \text{(Equation S1)}$$

where M_w is the molecular weight, N_A is the Avogadro number and Rg is the radius of gyration.

Representative examples of the normalized field autocorrelation functions:
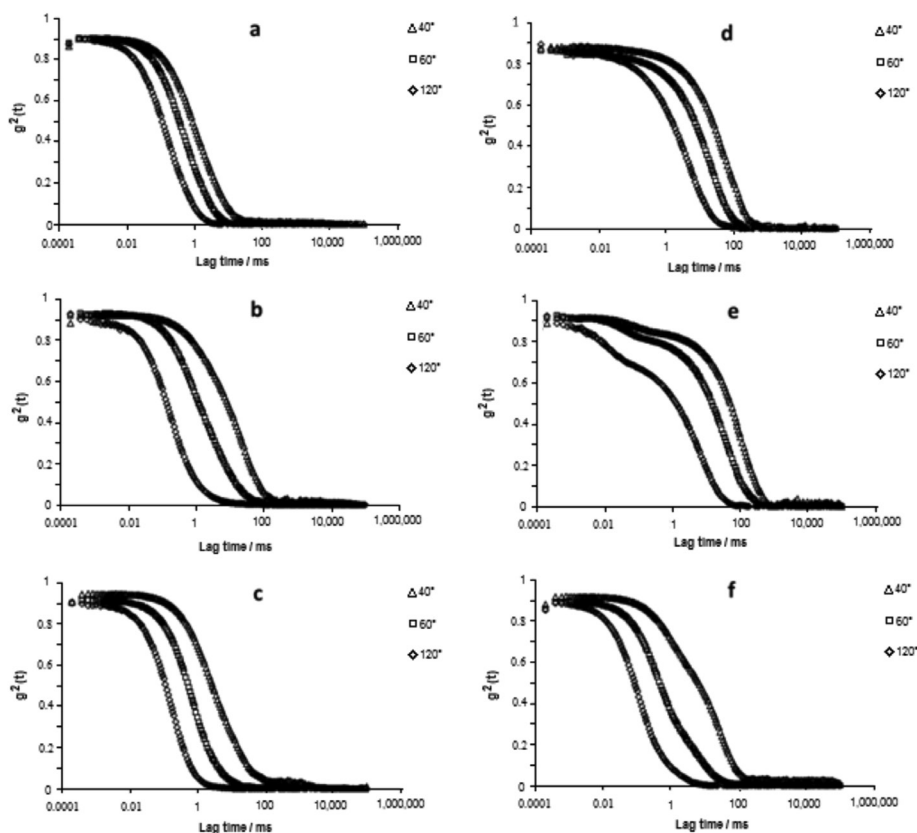
Figure S1. Normalized autocorrelation functions for (a), (b) and (c) PAHM-0 and (d), (e) and (f) PAHM-21, at ionic strength of (a) and (d) 0; (b) and (e) 2.7×10^{-3} (9.0×10^{-4} CaCl$_2$); (c) and (f) 2.0×10^{-1} mol L^{-1} (2.0×10^{-1} NaCl). Polymer concentration: 2 g L^{-1}.

*e-mail: balaban@supercabo.com.br

Dependence of Γ on q^2 for PAHM-0 in absence of salt. (a) fast mode and (b) slow mode. Full symbols indicate the data used to calculate the $D_{q\to0}$:
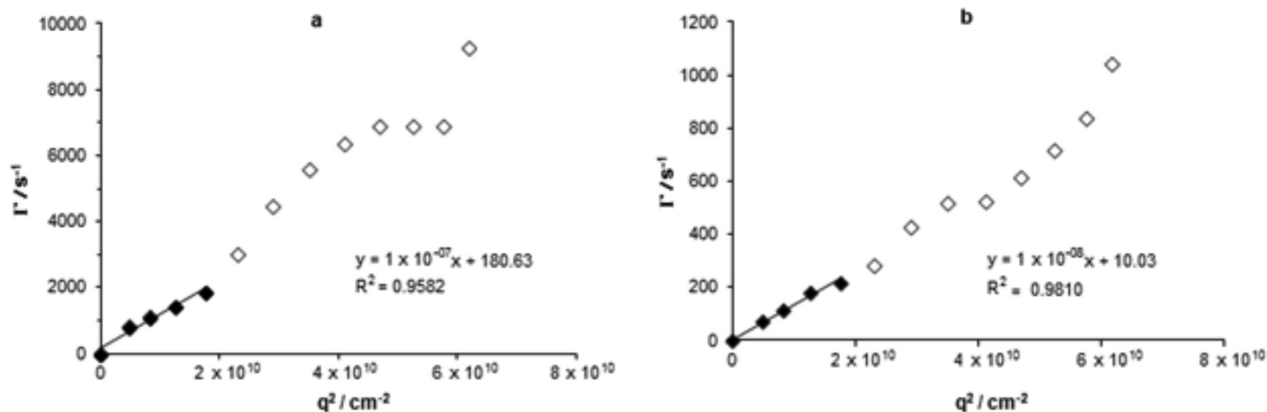

Figure S2. Dependence of G on q^2 for PAHM-0 at 2 g L^{-1} in distilled water: (a) fast mode and (b) slow mode.

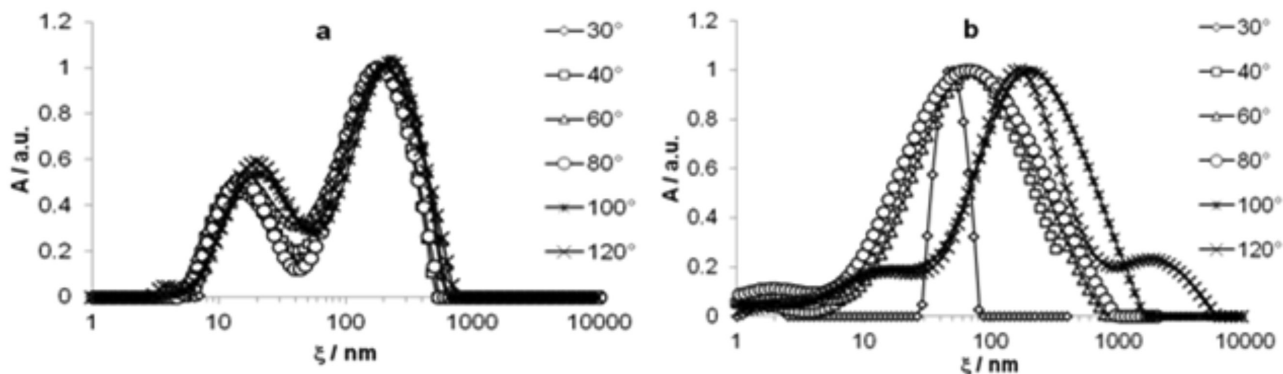**Figure S3**. Correlation length distributions as a function of the scattering angle for (a) PAHM-0 and (b) PAHM-21, at 2 g L^{-1} in distilled water.

The nominal wall shear rate in capillary viscometers may be calculated using the following equation:

$$\dot{y}_{wn} = \frac{32Q}{\pi D^3} \qquad \text{(Equation S2)}$$

where Q is the flow rate and D is the capillary diameter. The values calculated to the solutions analyzed in this work are between 1259 s^{-1} and 2269 s^{-1}.